Classical molecular dynamics simulation of microwave heating of liquids: the case of water

Classical molecular dynamics simulation of microwave heating of liquids: the case of water

N. D. Afify[1, a)] and M. B. Sweatman[1]

School of Engineering, The University of Edinburgh, The King's Buildings, Sanderson Building, Mayfield Road, Edinburgh EH9 3JL, United Kingdom

(Dated: 13 December 2017)

We perform a complete classical molecular dynamics study of the dielectric heating of water in the microwave region. MW frequencies ranging from 1.0 to 15.0 GHz are used together with a series of well-known empirical force fields. We show that the ability of an empirical force field to correctly predict the dielectric response of liquids to MW radiation should be evaluated on the basis of a joint comparison of the predicted and experimental static dielectric constant, frequency-dependent dielectric spectra, and heating profiles. We argue this is essential when multicomponent liquids are studied. We find that both the three-site OPC3 and four-site TIP4P-ϵ empirical force fields of water are equally superior for reproducing dielectric properties at a range of MW frequencies. Despite its poor prediction of the static dielectric constant, the well-known SPCE force field can be used to accurately describe dielectric heating of water at low MW frequencies.

Keywords: Classical molecular dynamics; Empirical force fields of water; Microwave heating of water; Dielectric spectra of water

[a)]Electronic mail: N.Afify@ed.ac.uk

I. INTRODUCTION

Dielectric heating of liquids using microwave (MW) radiation (0.3-300 GHz) is becoming an increasingly important research area, where many applications are emerging. One of these applications is the use of MW dielectric heating in the CO_2 capture process. Some of us have recently demonstrated the feasibility of regenerating spent amine solution using MW irradiation[1]. It was shown that MW heating can regenerate spent aqueous monoethanolamine solutions at lower temperatures than conventional thermal regeneration. Thus, the use of MW heating in CO_2 capture processes can potentially reduce their overall cost. To fully benefit from the advantages of MW heating, details of the dielectric response of these liquids to MW irradiation is required. Thus, an accurate determination of frequency-dependent dielectric spectra of liquids in the MW region is required.

Classical molecular dynamics (MD) is a very powerful computational technique able to characterize the dielectric properties of liquids though the prediction of static dielectric constants, frequency-dependent dielectric spectra, and dielectric heating profiles. This atomistic simulation technique is, in principle, able to provide atomic-scale details of the dielectric response of different components of liquid mixtures to MW radiation. Since the force field is the main ingredient of any classical MD study, the accuracy of the obtained dielectric properties is strongly dependent on the quality of the employed force field. This becomes more challenging in the case of multicomponent liquids where transferability of empirical force fields is not guaranteed.

Despite its great importance, a completely consistent methodology for using classical MD to simulate MW heating of liquids has, to our knowledge, yet to be developed. Some of us recently reported the frequency-dependent dielectric spectra of water, alcohols, glycols, and monoethanolamine using classical MD simulations[2]. In that study, several empirical force fields for each liquid were employed in an attempt to accurately predict their dielectric spectra. It was found that most of the tested empirical force fields failed to accurately predict experimental data. The main problem was inaccurate prediction of the static dielectric constant, which enters the frequency-dependent dielectric spectra calculation as a scaling factor, and which then influences predicted heating rates. The authors concluded that using the experimentally available values of static dielectric constants in the determination of dielectric spectra from MD results would be a reasonable alternative. Obviously, this procedure is

This manuscript was accepted by J. Chem. Phys. Click here to see the version of record.

not possible in the case of arbitrary mixtures of these liquids, for which experimental static dielectric constants are not yet available. Nor is it entirely consistent, since non-equilibrium molecular dynamics simulations of the heating rate would give inconsistent results.

In this work we report a comprehensive classical MD study of the dielectric heating of water, using MW radiation at frequencies ranging from 1.0 to 15.0 GHz and eight different empirical force fields. Their performance in predicting the static dielectric constant, frequency-dependent dielectric spectra, and frequency-dependent MW heating profiles for liquid water are reported. We show that reasonable agreement between all these predicted and experimental properties are required to justify their use in MD studies of the MW heating of multicomponent liquids.

II. COMPUTATIONAL DETAILS

Molecular dynamics simulations were carried out using the Large-scale Atomic/ Molecular Massively Parallel Simulator (LAMMPS) code[3]. The computational work was carried out on the Archer and Cirrus High Performance Computing (HPC) clusters available at the Edinburgh Parallel Computing Centre (EPCC) located at the University of Edinburgh. We selected the following frequently used three and four-site empirical force fields of water: (i) SPC[4], (ii) SPCE[5], (iii) TIP3P-Ew[6], (iv) TIP4P-2005[7], (v) TIP4P-Ew[7], (vi) OPC3[8], (vii) SWM4-NDP[9], and (viii) TIP4P-ϵ[10]. Unlike all the other evaluated force fields, SWM4-NDP is a polarizable water force field based on classical Drude oscillators[9]. It should be mentioned that our selection of these force fields was based mostly on their popularity. Although this work concerns only liquid water, the methodologies and approaches adopted are in principle applicable to other liquid systems.

For each empirical force field four different sets of classical MD simulations are carried out. All simulations employed 3000 water molecules in a cubic simulation box. This sample size was decided on the basis of the size-dependence of the different dielectric properties obtained from exploratory simulations. A time step of 1.0 fs was used for all simulations, with periodic boundary conditions (PBC) applied in all directions to mimic 3D bulk samples. Long-range Coulombic interactions were evaluated using the particle-particle/particle-mesh (PPPM) solver[3], using a precision factor of 0.0001 and a real space cut-off of 10.0 Å. The short-range interaction cut-off was set also to 10.0 Å. For all simulations bonds involving

hydrogen atoms were constrained during dynamics using the Shake algorithm[11] to allow for using a time step of 1.0 fs. All simulations were conducted at 298.0 K and 1 atmosphere of pressure. In the case of the SWM4-NDP polarizable force field the temperature of Drude particles was kept as low as 1.0 K in order to maintain the induced dipoles near the self-consistent induction regime[9].

The first set of MD simulations aimed to generate fully equilibrated samples to feed to the remaining sets of simulations. First, we energy-minimized the geometry of the starting atomistic configurations prior to the equilibration stage. Samples were then equilibrated at 298.0 K and atmospheric pressure for 2 ns. This period comprised NVT simulation for the first 0.1 ns and NPT simulation for the next 1.9 ns. During these simulations the temperature and pressure were controlled by the MTK[12] thermostat and barostat employing temperature and pressure damping factors of 0.1 ps and 1.0 ps respectively. The resulting final atomistic configurations were used as starting ones for the remaining three MD simulations sets.

The second set of MD simulations comprised equilibrium NVT simulations to determine the static dielectric constant from the total dipole moment induced in the sample by an external static electric field[13]. In these simulations electric fields with strengths ranging from 0.0 to 0.01 V/Å, with a step of 0.001 V/Å, were applied in the x direction. At each field strength samples were equilibrated for 200 ps. Temperature was controlled by the Nosé-Hoover thermostat[14] using a temperature damping factor of 0.1 ps. The total dipole moment of the simulation box was computed from the final 40 ps. The above procedure was repeated by applying an external static dielectric field in the y and z directions. The relation between the electric field strength and the induced average total dipole moment was fitted linearly to obtain the static electric constant.

At this point, it is useful to comment on the current implementation of the TIP4P force field in LAMMPS[3]. When we used the "pair_style lj/cut/tip4p/long" command in LAMMPS we obtained incorrect results for the TIP4P-2005, TIP4P-Ew, and TIP4P-ϵ force fields whenever an external electric field was present. We found that the applied electric field does not take into account the presence of the fourth massless site in the TIP4P models. To solve this problem we declared the massless site explicitly in LAMMPS input and used the general "pair_style lj/cut/long" command.

The third set of MD simulations comprised equilibrium NVT MD simulations to determine the static dielectric constant from the magnitude of fluctuations in the total dipole

This manuscript was accepted by J. Chem. Phys. Click here to see the version of record.

ngment[15], following the same method as previous work[2]. According to Neumann's formula the static dielectric constant is related to the magnitude of fluctuations of the total dipole moment (i.e. $\langle M.M\rangle - \langle M\rangle . \langle M\rangle$) by Equation 1.

$$\varepsilon_o = \varepsilon_\infty + \frac{4\pi}{3k_BTV}(\langle M.M\rangle - \langle M\rangle . \langle M\rangle) \quad (1)$$

In equation 1, k_B, T, V, and ε_∞ represent the Boltzmann constant, system temperature and volume, and high-frequency dielectric constant. Our calculations confirmed that the term $\langle M\rangle . \langle M\rangle$ is negligible. During these NVT simulations temperature was controlled by the Nosé-Hoover thermostat using a damping factors of 0.1 ps. For each force field a trajectory of 20 ns was simulated and the total dipole moment of the system was recorded each 1, 10, and 100 fs. The obtained trajectories were also used in computing the frequency-dependent dielectric spectra, as explained later.

Finally, in the fourth set of MD simulations we performed non-equilibrium dielectric heating studies of water in the MW region at the following MW frequencies: 1.0, 2.45, 5.8, 10.0, and 15.0 GHz. This set of simulations utilized the NVE ensemble. At each frequency an external electric field, with cosine waveform, was applied along the x direction with amplitude set to 0.01 V/Å. Initial testing confirmed that this field strength is within the linear response regime for these water models. For each MW frequency ten complete electric field cycles were simulated. The average system temperature was recorded at each 0.1 ps.

To obtain the rise in temperature due to the presence of the external electric field the following procedure was adopted. First, the temperature trajectory in the absence of an electric field was linearly fitted. The resulting linear behavior was then subtracted from each temperature trajectory in the presence of an electric field. The resulting curves represent therefore the rise in system temperature due only to the applied external electric field. These heating curves were linearly fitted and the predicted heating rate at each MW frequency was calculated. The above procedure was independently repeated two times by applying the electric field along the y and z directions. From these three independent heating simulation sets the average heating rates and their standard deviations were computed and compared to experiment.

III. RESULTS AND DISCUSSION

In this section we present and discuss our different sets of results, aiming to illustrate a general and consistent methodology to study microwave heating of liquids using the classical MD technique. Results for the static dielectric constant of water are presented first, followed by the frequency-dependent dielectric spectra. Finally, we present the predicted heating profiles for water at different MW frequencies. Finally, an overall conclusion will be made based on all the obtained results.

As described above, the static dielectric constant of water was calculated using two different approaches. Figure 1 of the Supplementary Material reports the dielectric constant of water calculated using Neumann's formula (equation 1). Results are reported in the case of the SPCE force field as an example, obtained using three different sampling frequencies of the total dipole moment. The cumulative average result for the dielectric constant is shown, illustrating convergence of the final result with increasing simulation time. The horizontal dotted line corresponds to the experimental value of static dielectric constant of water[16]. Our second method for determination of the static dielectric constant involves equilibration under an applied electric field[17]. Figure 2 of the Supplementary Material shows an example set of results, reported in the case of the SPCE force field. The response appears to be in the linear regime.

Figure 1 compares the experimental (horizontal dotted line) static dielectric constant of water[16] with the values predicted by these two different simulation routes for each force field used. From this figure it is clear that static dielectric constants predicted by both simulation routes agree well with each other. The superior quality of the recently developed 3-point Optimal Point Charge (OPC3) force field[8] is evidenced by the excellent agreement with experiment. Next to OPC3 comes the four-site TIP4P-ϵ force field[10]. We tested different system sizes and short-range cutoffs, and found these results to be insensitive to these details.

We obtained the following average values of the static dielectric constant of water: 67.1 $\pm$ 2.2 (SPC), 72.4 $\pm$ 2.1 (SPCE), 91.9 $\pm$ 2.0 (TIP3P-Ew), 79.3 $\pm$ 1.9 (OPC3), 58.8 $\pm$ 1.6 (TIP4P-2005), 65.8 $\pm$ 2.1 (TIP4P-Ew), 77.9 $\pm$ 2.0 (TIP4P–ϵ), 75.5 $\pm$ 2.0 (SWM4-NDP). Our results agree well with the following computational studies: 65.0 (SPC[18]), 71.0 (SPCE[5]), 89.0 (TIP3P-Ew[6]), 78.4 (OPC3[8]), 60.0 (TIP4P-2005[7]), 63.4 (TIP4P-Ew[7]), 78.3 (TIP4P-ϵ[10]), and 79.0 (SWM4-NDP[9]).

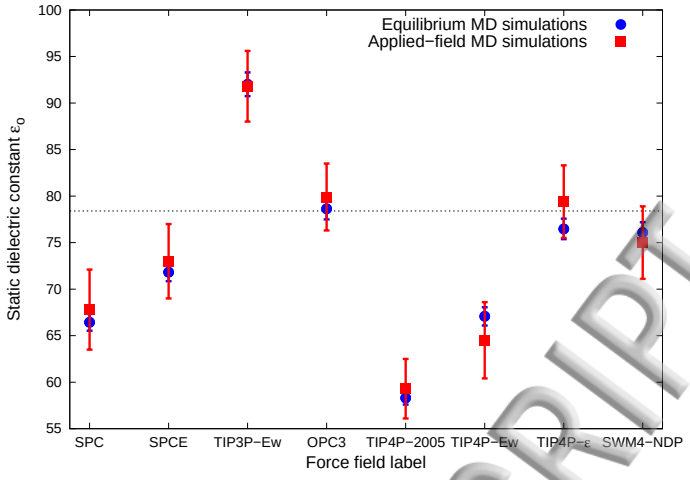

FIG. 1. Comparison between the experimental static dielectric constant of liquid water (horizontal dotted line)[16] and the static dielectric constants predicted by the different empirical force fields employing both equilibrium (blue spheres) and applied-field (red squares) MD simulations.

Now we move on to the ability of the different empirical force fields to correctly predict the frequency-dependent dielectric spectra of water, particularly in the MW region. The dielectric spectra predicted by each force field were calculated using the following procedure. The total dipole moment autocorrelation function was fitted to an exponential decay function to determine the relaxation time (τ_D). The fitting process was carried out using the GROMACS g_dielectric analysis tool[19]. Figure 3 of the Supplementary Material demonstrates an example of such fitting in the case of the SPCE force field. The determined relaxation time was then used to calculate the real and imaginary parts of the frequency-dependent dielectric spectra using the Debye relaxation model[20] in the frequency range form 0.001 to 600.0 GHz. According to this model the real and imaginary parts of the dielectric spectrum are given by Equations 2 and 3. In these calculations an experimental value of the high-frequency dielectric constant ($\varepsilon_\infty = 1.76$[21,22]) of water was used.

$$\varepsilon_{Re}(\omega) = \varepsilon_\infty + \frac{\varepsilon_o - \varepsilon_\infty}{1 + \omega^2 \tau_D^2} \tag{2}$$

$$\varepsilon_{Im}(\omega) = \frac{(\varepsilon_o - \varepsilon_\infty)\omega\tau_D}{1 + \omega^2 \tau_D^2} \tag{3}$$

In Figure 2 the real (Figure 2(a)) and imaginary (Figure 2(b)) parts of the frequency-dependent dielectric spectra of water as predicted by the different empirical force fields (solid

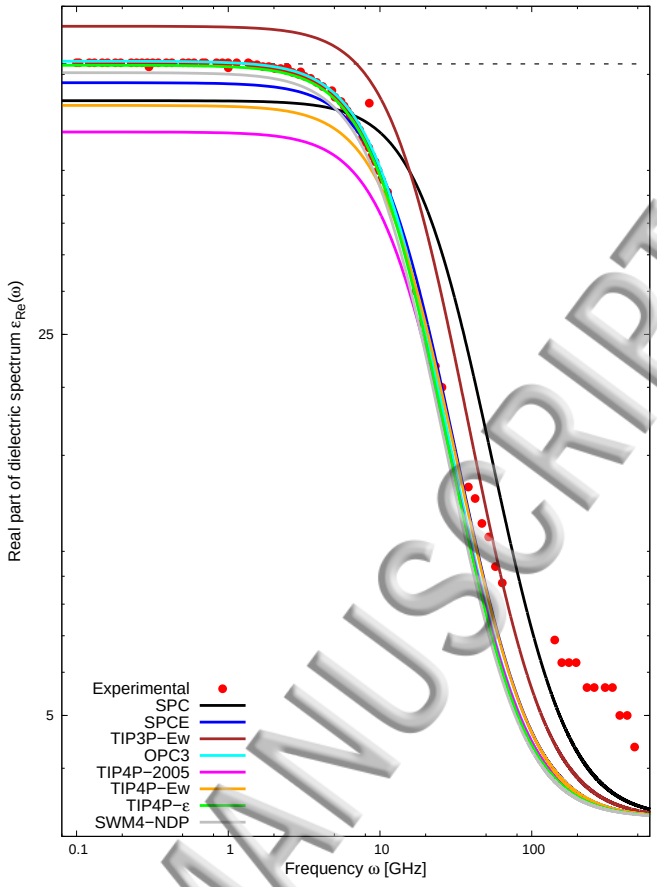

(a)

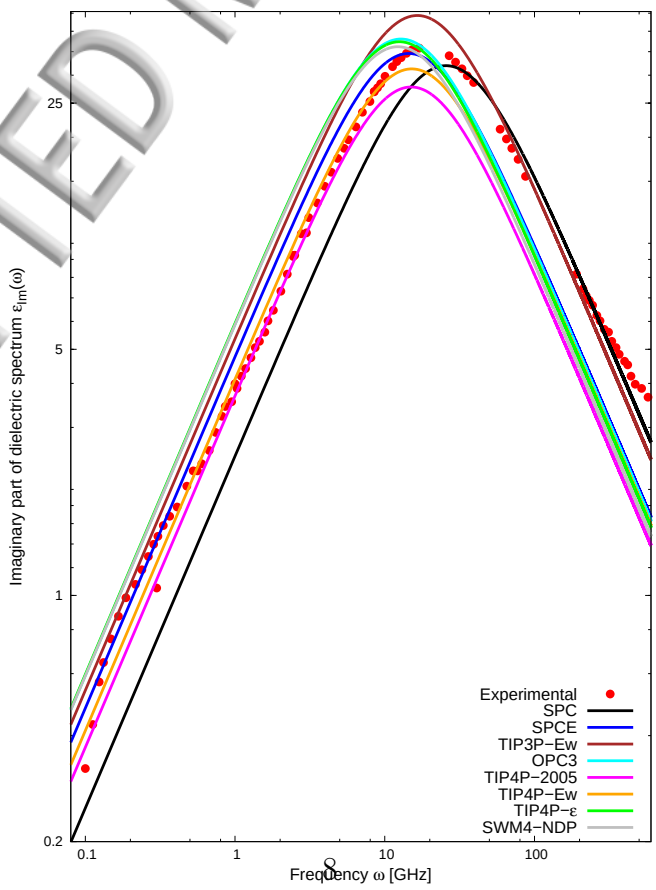

(b)

lines) are compared to their experimental counterparts (red dots)[23–26]. The horizontal dotted line in figure 2(a) corresponds to the experimental static dielectric constant of water[16]. It should be emphasized that the static dielectric constants employed in the calculation of these dielectric spectra were obtained by averaging the values obtained from our equilibrium and applied-field MD simulations for each force field.

The task now is to identify the best empirical force field able to reproduce the experimental real and imaginary parts of the frequency-dependent dielectric spectrum of water. Inspection of figure 2(a) reveals that the real part is best predicted by the OPC3 force field (cyan line) up to 20 GHz, i.e. in the most relevant region for our study. The TIP4P-ϵ force field (green line) is next best. Figure 2(b) reveals that the OPC3 and TIP4P-ϵ are not the best force fields able to reproduce the imaginary part of the experimental dielectric spectrum of water. In fact the SPCE force field (blue line) shows slightly better quality. Furthermore, TIP3P-Ew (brown line) is the only force field able to correctly predict the experimental position of the main loss peak. From figures 2(a) and 2(b) it can be concluded that none of the tested force fields was able to accurately predict both the real and imaginary parts of the experimental dielectric spectrum of water. At this point, it is not possible to decide which force field we should select if we would like to study the MW dielectric heating of water.

Both the real and imaginary part of the dielectric spectrum are important for studying the MW dielectric heating. While the real part is related to the ability of material to absorb and store the MW energy, the imaginary part is related to the ability of material to dissipate the stored MW energy into other forms such as heat[27]. We will show later that further MD calculations are required to be able to compare the average performance of the different empirical force fields in describing the dielectric response of water to MW radiation.

Due to the inability of most available empirical force fields to accurately predict the dielectric response of liquids, Cardona et al.[2] suggested using the experimental values of static dielectric constants when computing the frequency-dependent dielectric spectra of these liquids using the Debye relaxation model[20]. Following this suggestion we used the experimental static dielectric constant of water to compute the dielectric spectra of water. A comparison between the experimental and calculated frequency-dependent dielectric spectra of water as predicted by the different empirical force fields is reported in Figure 4 of the Supplementary Material. It can be seen from this figure, a part from the SPC force field,

that most of the tested empirical force fields are able to reasonably predict the experimental dielectric spectra, and it is not so clear which should be selected. Obviously this approach is not applicable in the case of liquid mixtures for which experimental static dielectric constants are not usually available.

However, in principle, if we wish to select a force field suitable for dielectric heating studies, it makes most sense to consider heating profiles generated by each model. In Figure 3 we report the predicted heating profiles (solid lines) caused by applying time-dependent external electric fields at MW frequencies ranging from 0.0 to 15.0 GHz. In this figure we report the results obtained using the SPCE force field as an example. To clearly visualize the dependence of heating profiles on MW frequency we included in figure 3 the linear fit for each heating profile (dotted lines). It should be noted that the black curve represents the temperature baseline, where no external electric field was applied. From this curve it is clear that there is no significant drift in temperature although we used the NVE ensemble. This confirms that the starting atomistic configurations used in our MD heating simulations are very well equilibrated, and thus any resulting rise in temperature can be entirely due to the effect of the applied external electric field. It is important to note that even for electric fields with the lowest frequency (1.0 GHz) our MD simulations are able to detect a heating effect, as is clearly seen when comparing the black and red dotted lines in figure 3.

As expected, figure 3 shows that the dielectric MW heating of water becomes more efficient when one utilizes MW radiation with higher frequencies. In fact, MW radiation with a frequency of 15.0 GHz is able to heat 3000 water molecules to 330 K in 0.7 ns time. It should be noted that such heating efficiencies are extremely high when compared to typical experimental heating efficiencies. This is due to the fact we applied electric fields with an extremely high amplitude (i.e. 0.01×10^{10} V/m) in order to be able to obtain accurate heating profiles in a reasonable MD simulation time.

To obtain MW heating rates at different MW frequencies we carried out linear fitting on the curves reported in figure 3 after the removal of the baseline temperature. The slope of the resulting straight line represents the heating rate in this case. To compare the predicted heating rates to the ones expected from experiment we followed the following procedure. For a microwave heating process in a closed system, assuming there are no chemical reactions or heat losses due to convection and conduction to the surroundings, conservation of energy leads to Equation 4.

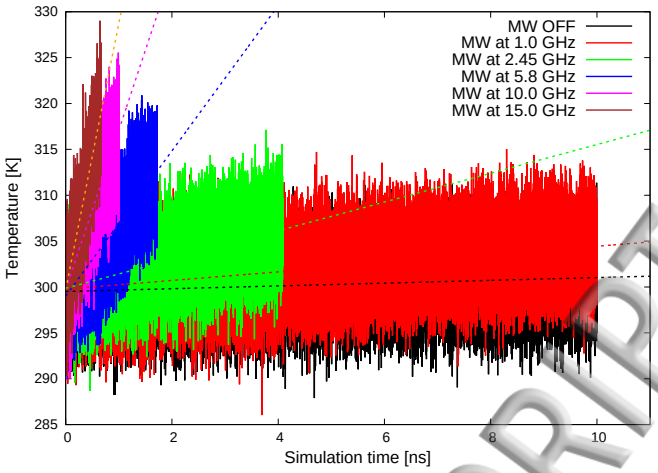

FIG. 3. The predicted classical MD heating profiles of water caused by applying time-dependent external electric fields at MW frequencies ranging from 1.0 to 15.0 GHz. Results are reported for the case of the SPCE force field as an example. The black curve represents the temperature baseline, where no external electric field was applied. The time length of each simulation corresponds to ten full electric field cycles. The dotted lines represent the linear fit for each heating profile.

$$mc_p(T)\frac{dT}{dt} = \omega\varepsilon_o\varepsilon_{Im}(\omega,T)|E(\omega)|^2V \tag{4}$$

In this equation m, V, $\frac{dT}{dt}$, and c_p are the simulation box mass and volume, heating rate, and the specific heat capacity of the material. ω, ε_o, $\varepsilon_{Im}(\omega,T)$, and $|E(\omega)|$ are the MW frequency, vacuum permittivity, imaginary part of dielectric spectrum at the frequency ω, and the root mean square amplitude of the applied external electric field.

Figure 4 reports a comparison between the experimental (solid red squares) and classical MD predicted (solid spheres) MW heating rates of water using the different empirical force fields. The experimental heating rates were calculated from equation 4 using solely experimental parameters. From this figure it can be seen that OPC3 and TIP4P-ϵ are the best two empirical force fields able to reproduce, with very similar qualities, the experimental heating rates at the different MW frequencies. Inspection of figure 4 reveals that the match between experimental and calculated heating rates at low MW frequencies, namely 1.0 and 2.45 GHz, is best predicted by the the SPCE force field. It is interesting to see that the SPCE force field can be used to accurately describe MW heating of water at low MW frequencies although it failed to predict the experimental static dielectric constant of water.

This manuscript was accepted by J. Chem. Phys. Click here to see the version of record.

From equation 4 it can be seen that the heat generated in atomistic simulations depend also on ability of the used force field to accurately predict the specific heat capacity of the liquid. Thus, a given force field might accurately reproduce static dielectric constant and dielectric spectra but it fails to predict accurate heating rates.

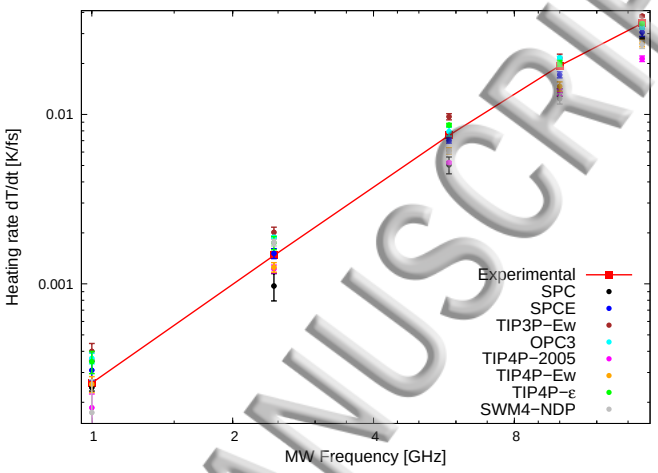

FIG. 4. Comparison between the experimental (solid red squares) and classical MD predicted (solid spheres) MW heating rates of water using the different empirical force fields. These heating simulations employed electric fields with an amplitude of 0.01 V/Å.

In real-world MW dielectric heating applications mixtures of different liquids are usually heated together. To understand and/or optimize the MW heating process detailed knowledge of the dielectric response of the different liquid components to MW irradiation is required. Achieving this goal requires the availability of accurate force fields that are able to accurately describe the dielectric response of the different liquid components to MW fields. The current study demonstrates that having an empirical force field that is able to reasonably reproduce experimentally observed frequency-dependent dielectric spectra does not guarantee an equivalent level of accuracy in the simulation of the heating process itself. Therefore, conventional force field validation procedures should be extended to assure that heating rates predicted by these force fields agree reasonably well with experiment at the relevant MW frequencies.

IV. CONCLUSIONS

In summary, we used a comprehensive classical molecular dynamics framework to evaluate the ability of some widely-used empirical force fields to accurately describe the dielectric response of liquid water to microwave irradiation at different microwave frequencies. The static dielectric constant, frequency-dependent dielectric spectra, and microwave heating rates for liquid water were calculated and compared to their experimental counterparts. It is found that all of these validation levels are necessary in order to identify an empirical force field that can be used in realistic microwave heating simulations of liquids. Following this thorough evaluation procedure it is found that both the TIP4P-ϵ and OPC3 force fields equally outperform all the other tested force fields, since the microwave heating rates predicted by these two force fields agree quantitatively with experiment at all the studied MW frequencies.

V. SUPPLEMENTARY MATERIAL

See supplementary material for the following extra figures: (1) Effect of equilibrium MD simulation length and dipole moment sampling interval on the predicted static dielectric constant of water, (2) An example of the linear fit of the relation between the total dipole moment and applied external electric field strength, (3) An example of the exponential fit of the total dipole moment autocorrelation function of water, and (4) Effect of using the experimental static dielectric constant of water in the calculation of frequency-dependent dielectric spectra on the agreement with experimental spectra.

ACKNOWLEDGMENTS

We are grateful for funding from the UK Engineering and Physical Sciences Research Council (EPSRC). We would like to thank Prof. X. Fan, Dr. J. Cardona, and Dr. F. Bougie for very useful discussions and comments.

REFERENCES

[1]S. J. McGurk, C. F. Martn, S. Brandani, M. B. Sweatman, and X. Fan, *Appl. Energy* **192**, 126 (2017).

[2]J. Cardona, R. Fartaria, M. B. Sweatman, and L. Lue, *Mol. Simul.***42**, 370 (2016).

[3]S. Plimpton, *J. Comput. Phys.***117**, 1 (1995).

[4]H. J. C. Berendsen, J. P. M. Postma, W. F. van Gunsteren, and J. Hermans, *J. Intermolecular forces. Dordrecht: Reidel D Publishing Company*, 331 (1981).

[5]H. J. C. Berendsen, J. R. Grigera, and T. P. Straatsma, *J. Phys. Chem.***91**, 6269 (1987).

[6]D. J. Price, and C. L. Brooks, *J. Chem. Phys.***121**, 10096 (2004).

[7]J. L. F. Abascal, C. Vega, *J. Chem. Phys.***123**, 234505 (2005).

[8]S. Izadi, and A. V. Onufriev, *J. Chem. Phys.***145**, 074501 (2016).

[9]G. Lamoureux, E. Harder, I. V. Vorobyov, B. Roux, and A. D. MacKerell Jr., *Chem. Phys. Lett.***418**, 245 (2006).

[10]R. Fuentes-Azcatl, and M. C. Barbosa, *Physica A***444**, 86 (2016).

[11]J. P. Ryckaert, G. Ciccotti, and H. J. C. Berendsen, *J. Comp. Phys.***23**, 327 (1977).

[12]M. E. Tuckerman, J. Alejandre, R. López-Rendón, A. L. Jochim, and G. J. Martyna, *J. Phys. A: Math. Gen.***39**, 5629 (2006).

[13]S. Floros, M. Liakopoulou-Kyriakides, K. Karatasos, and G. E. Papadopoulos, *Xu B., ed. PLoS ONE***12**, 1 (2017).

[14]W. G. Hoover, *Phys. Rev. A***31**, 1695 (1985).

[15]M. Neumann, and O. Steinhauser, *Chem. Phys. Lett.***102**, 508 (1983).

[16]G. Gente, and C. La Mesa, *J. Solution Chem.***29**, 1159 (2000).

[17]J. Kolafa, and L. Viererblová, *J. Chem. Theory Comput.***10**, 1468 (2014).

[18]D. van der Spoel, P. J. van Maaren, and H. J. C. Berendsen, *J. Chem. Phys.***108**, 10220 (1998).

[19]B. Hess, C. Kutzner, D. van der Spoel, and E. Lindahl, *J. Chem. Theory Comput.***4**, 435 (2008).

[20]A. M. Holtzer, *J. Polym. Sci.***13**, 548 (1954).

[21]R. J. Sengwa, V. Khatri, and S. Sankhla, *Proc. Indian Natn. Sci. Acad***74**, 67 (2008).

[22]R. J. Sengwa, V. Khatri, and S. Sankhla, *J. Solution Chem.***38**, 763 (2008).

[23]U. Kaatze, and V. Uhlendorf, *Z. Phys. Chem. Neue. Fol.***126**, 151 (1981).

[24]U. Kaatze, *J. Chem. Eng. Data.***34**, 371 (1989).

[25]J. Barthel, K. Bachhuber, R. Buchner, and H. Hetzenauer, *Chem. Phys. Lett.***165**, 369 (1990).

[26]J. B. Hasted, and S. H. M. El Sabeh, *T. Faraday Soc.***49**, 1003 (1953).

[27]C. Talens, M. Castro-Giraldez, and P. J. Fito, *LWT-Food Sci. Technol.***66**, 622 (2016).

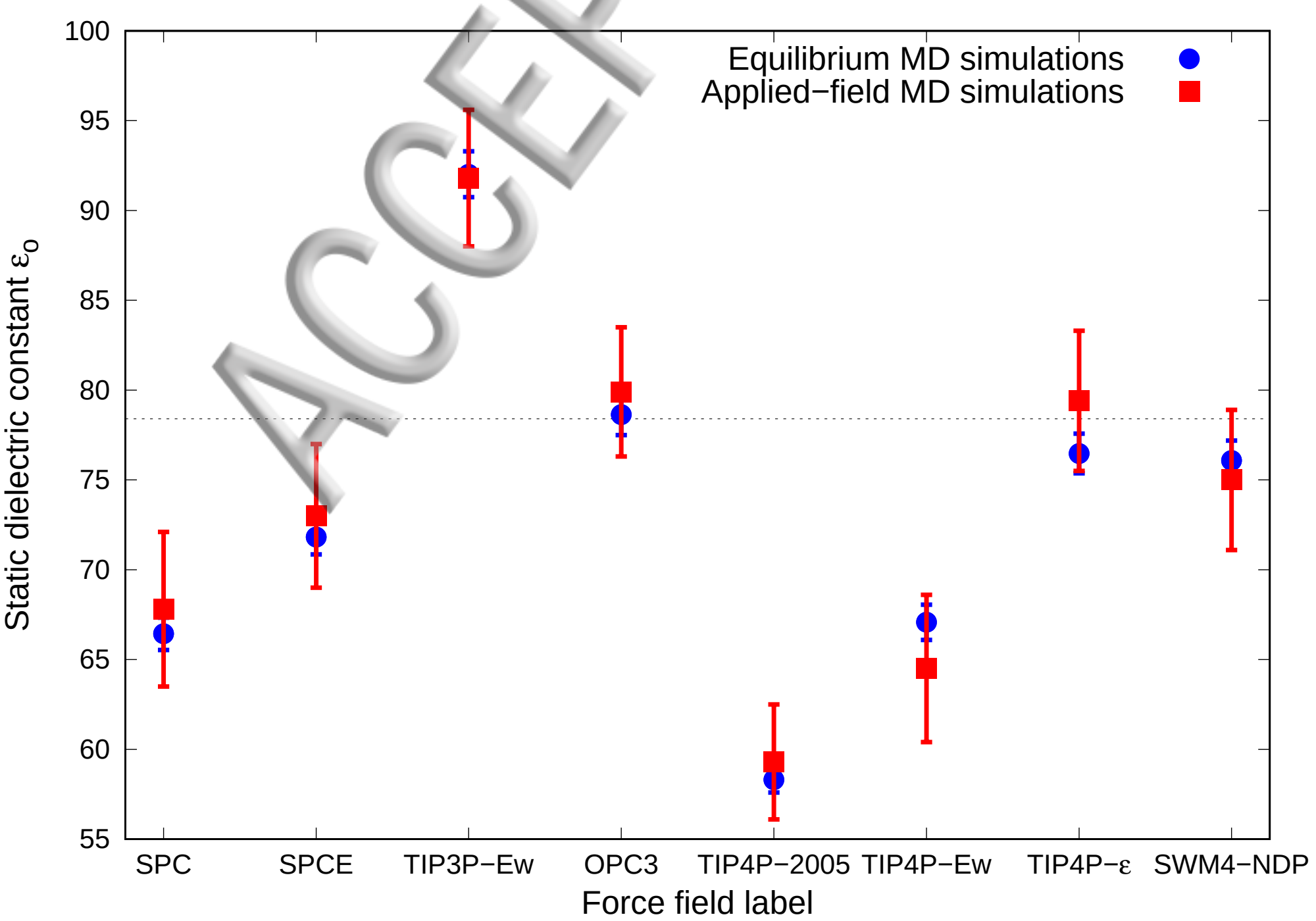
Equilibrium MD simulations
Applied−field MD simulations
Static dielectric constant ε_0
100
95
90
85
80
75
70
65
60
55
SPC
SPCE
TIP3P−Ew
OPC3
TIP4P−2005
TIP4P−Ew
TIP4P−ε
SWM4−NDP
Force field label

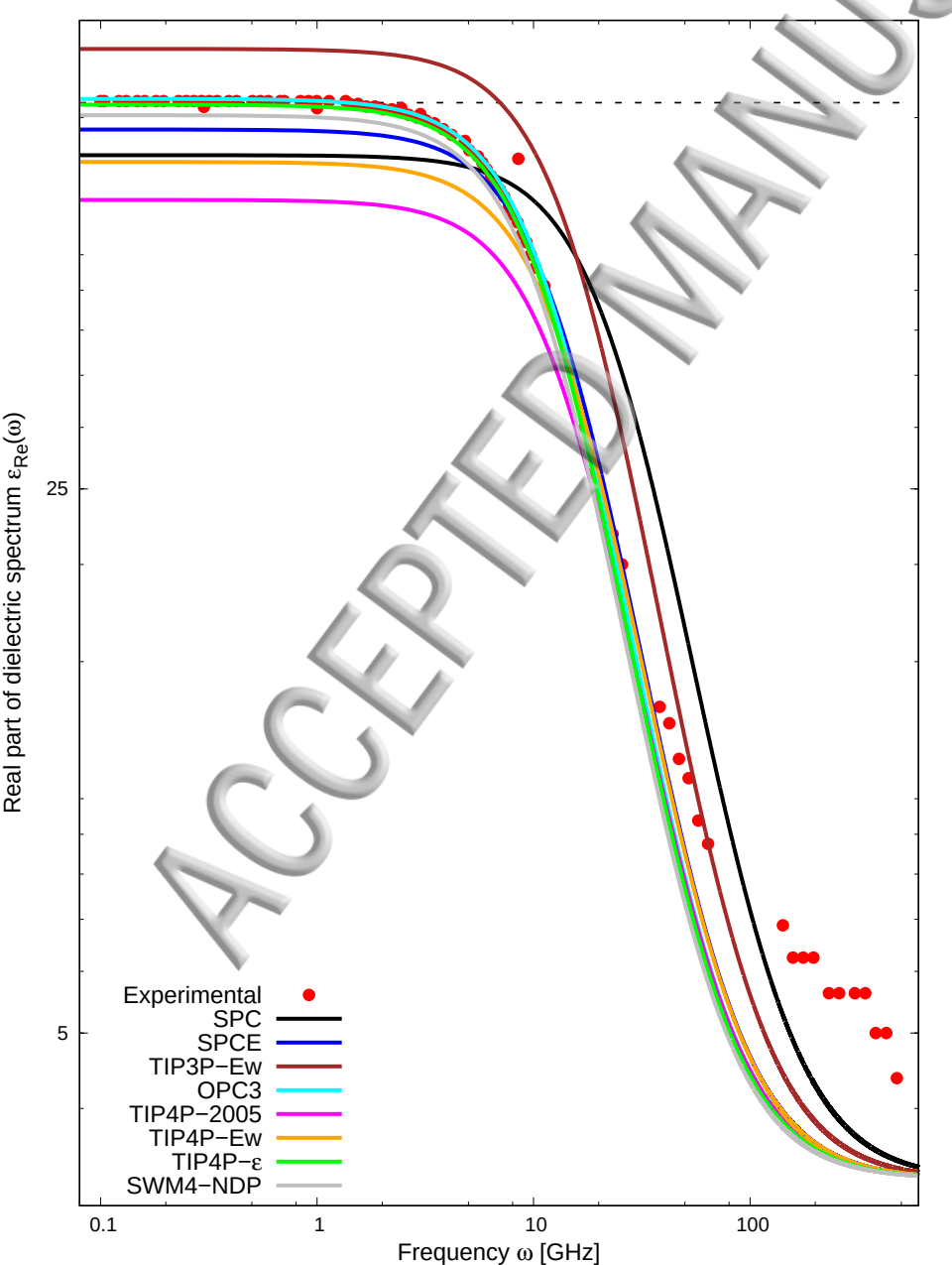

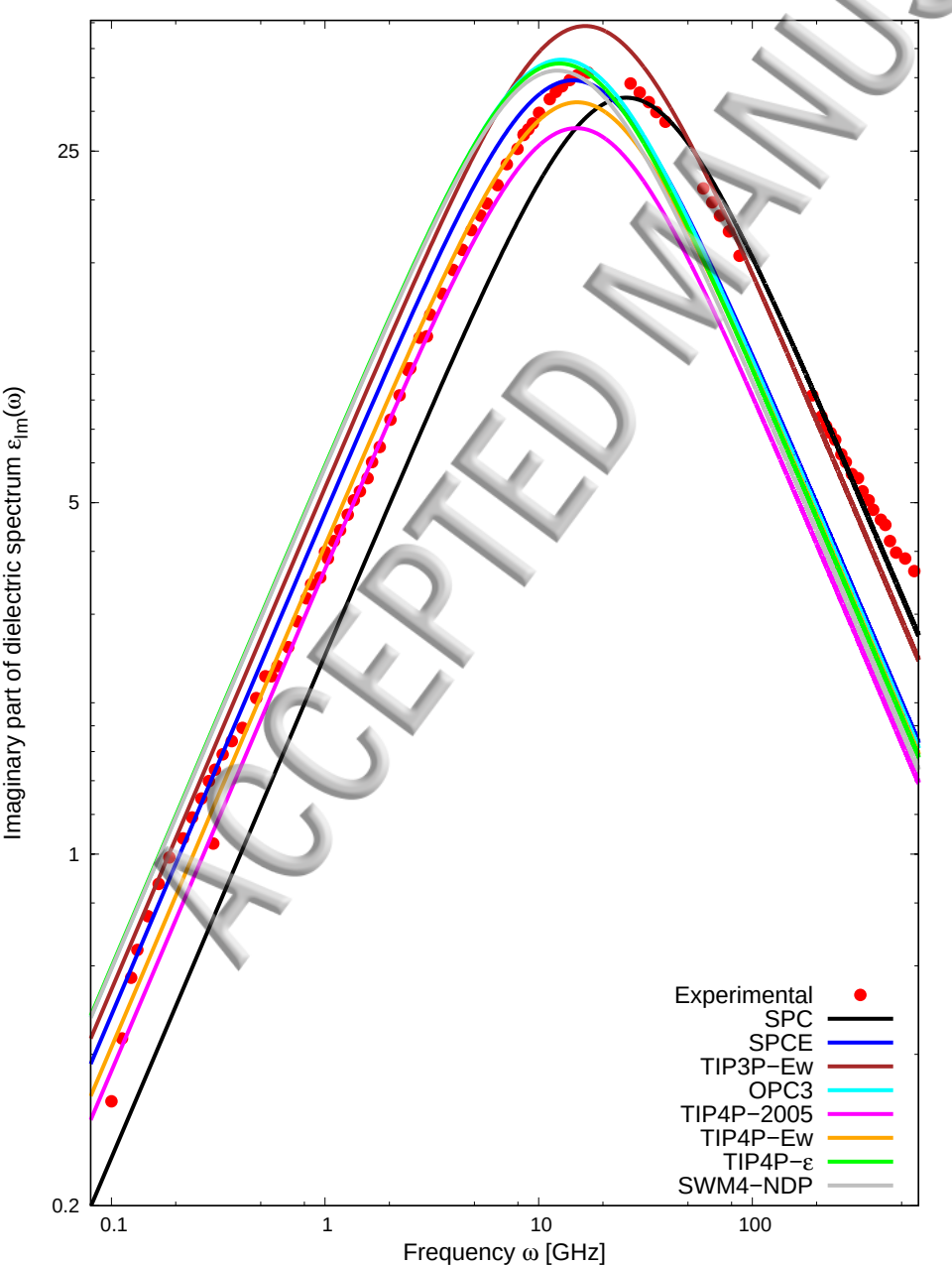

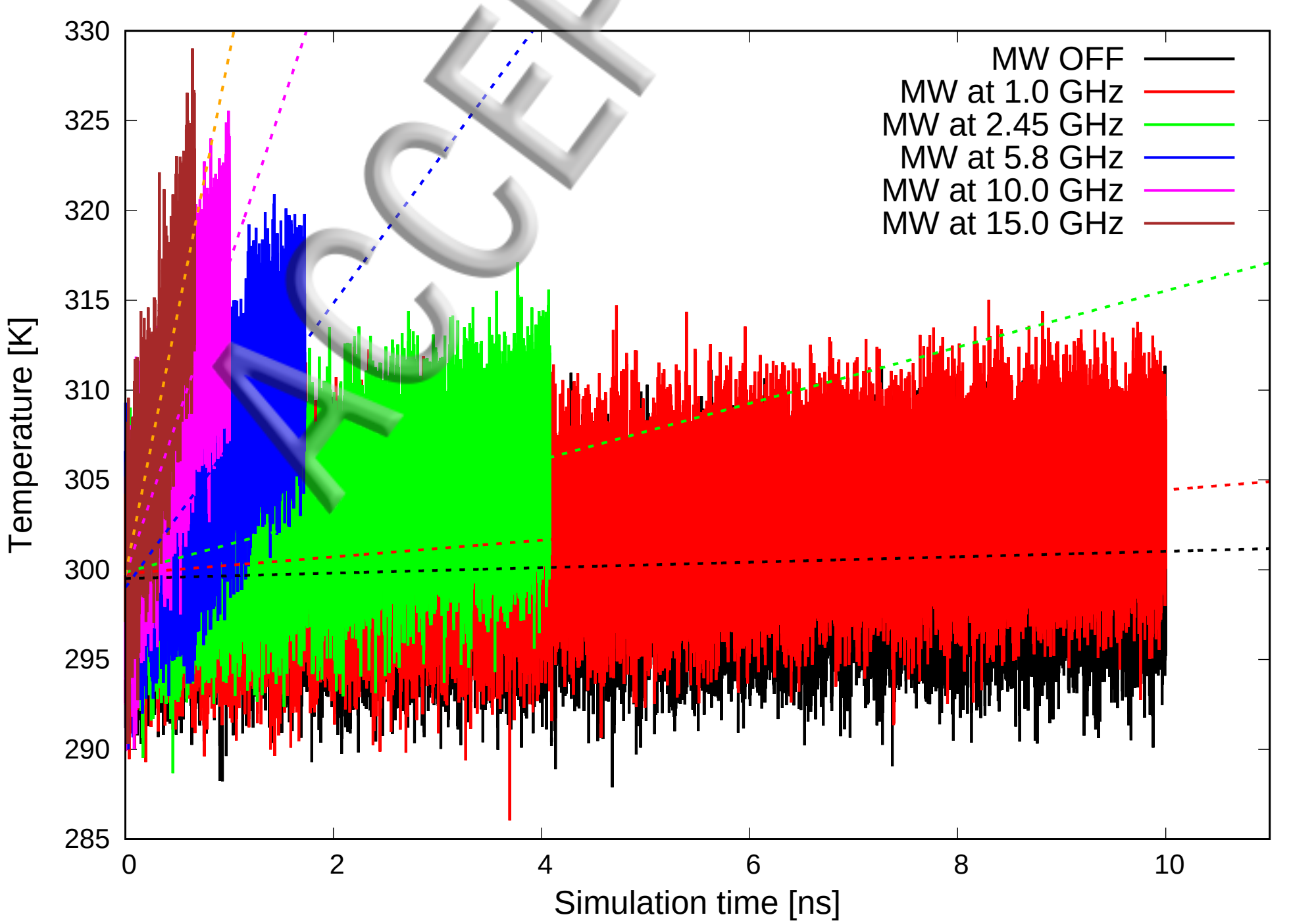
MW OFF
MW at 1.0 GHz
MW at 2.45 GHz
MW at 5.8 GHz
MW at 10.0 GHz
MW at 15.0 GHz
Temperature [K]
330
325
320
315
310
305
300
295
290
285
0
2
4
6
8
10
Simulation time [ns]

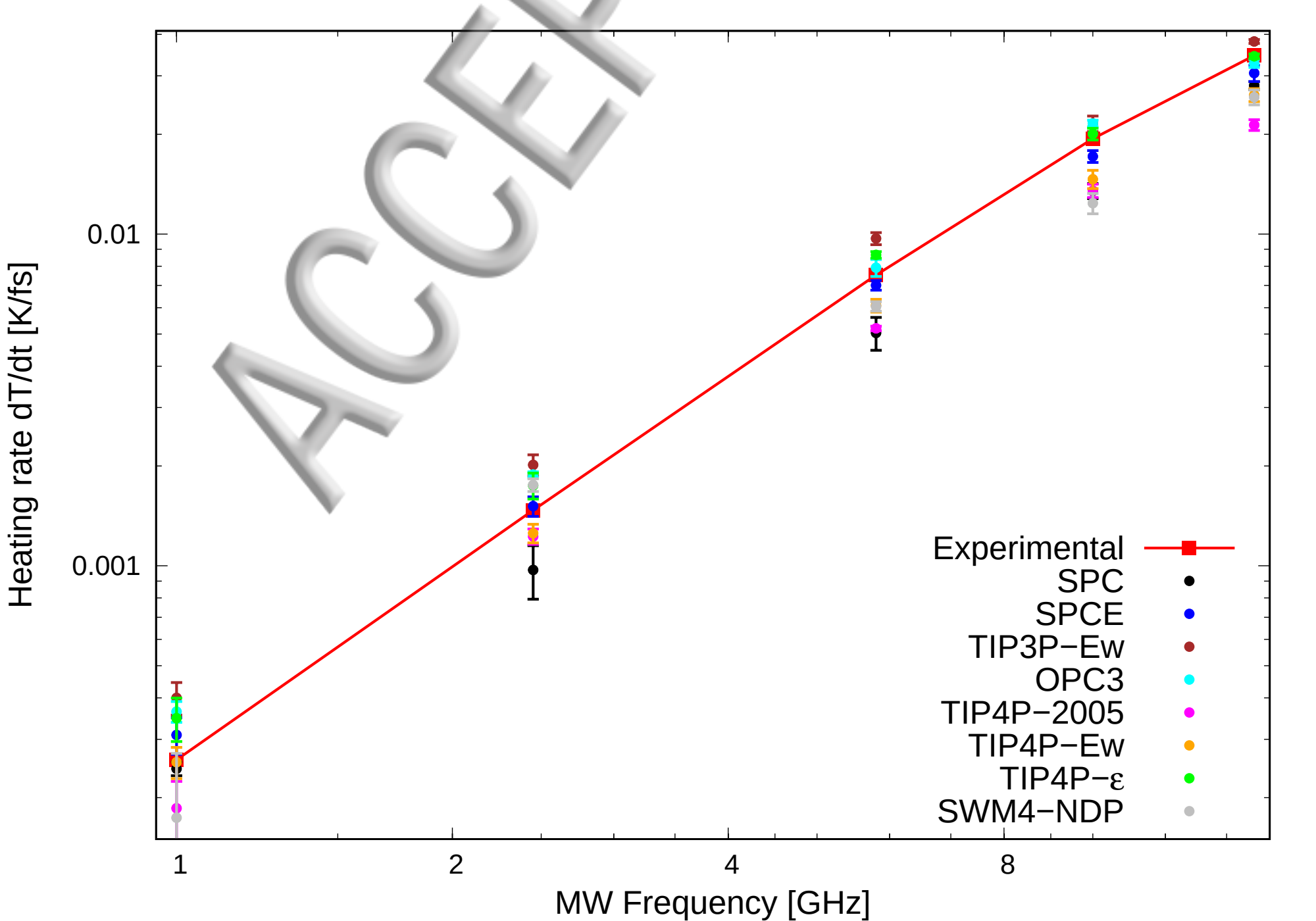
Heating rate dT/dt [K/fs]
0.01
0.001
1
2
4
8
MW Frequency [GHz]
Experimental
SPC
SPCE
TIP3P−Ew
OPC3
TIP4P−2005
TIP4P−Ew
TIP4P−ε
SWM4−NDP